physical sciences forum

Proceeding Paper

Reconstruction, Analysis and Constraints of Cosmological Scalar Field ϕCDM Models

Olga Avsajanishvili and Lado Samushia

MDPI

https://doi.org/10.3390/ECU2023-14060

physical sciences forum

MDPI

Proceeding Paper

Reconstruction, Analysis and Constraints of Cosmological Scalar Field ϕCDM Models †

Olga Avsajanishvili [1,2,*] and Lado Samushia [1,3]

1 E. Kharadze Georgian National Astrophysical Observatory, 0179 Tbilisi, Georgia
2 School of Natural Sciences and Medicine, Ilia State University, 3/5 Cholokashvili Ave., 0162 Tbilisi, Georgia
3 Department of Physics, Kansas State University, 116 Cardwell Hall, Manhattan, KS 66506, USA
* Correspondence: olga.avsajanishvili@iliauni.edu.ge
† Presented at the 2nd Electronic Conference on Universe, 16 February–2 March 2023; Available online: https://ecu2023.sciforum.net/.

Abstract: We studied the following scalar field ϕCDM models: ten quintessence models and seven phantom models. We reconstructed these models using the phenomenological method developed by our group. For each potential, the following ranges were found: (i) model parameters; (ii) EoS parameters; and (iii) the initial conditions for differential equations, which describe the dynamics of the universe. Using MCMC analysis, we obtained the constraints of scalar field models by comparing observations for the expansion rate of the universe, the angular diameter distance and the growth rate function, with corresponding data generated for the fiducial ΛCDM model. We applied Bayes statistical criteria to compare scalar field models. To this end, we calculated the Bayes factor, as well as the *AIC* and *BIC* information criteria. The results of this analysis show that we could not uniquely identify the preferable scalar field ϕCDM models compared to the fiducial ΛCDM model based on the predicted DESI data, and that the ΛCDM model is a true dark energy model. We investigated scalar field ϕCDM models in the w_0–w_a phase spaces of the CPL-ΛCDM contours. We identified subclasses of quintessence and phantom scalar field models that, in the present epoch: (i) can be distinguished from the ΛCDM model; (ii) cannot be distinguished from the ΛCDM model; and (iii) can be either distinguished or undistinguished from the ΛCDM model. We found that all the studied models can be divided into two classes: models that have attractor solutions and models whose evolution depends on initial conditions.

Keywords: dark energy; scalar field; large-scale structure; Bayesian statistics; Monte Carlo Markov chain analysis

Citation: Avsajanishvili, O.; Samushia, L. Reconstruction, Analysis and Constraints of Cosmological Scalar Field ϕCDM Models. *Phys. Sci. Forum* **2023**, *7*, 26. https://doi.org/10.3390/ECU2023-14060

Academic Editor: Gonzalo Olmo

Published: 18 February 2023

1. Introduction

According to measurements of supernova type Ia magnitudes, the expansion of our universe is accelerating [1,2]. One of the possible explanations for this fact is that the energy density of the universe is dominated by so-called dark energy, a component with effective negative pressure [3]. The simplest description of dark energy is the concept of vacuum energy or the cosmological constant Λ [4]. The energy density of the cosmological constant does not depend on time and has recently become dominant (in particular, the energy density associated with the cosmological constant is about 69% of the total energy density of the universe in the present epoch [5]). Sometimes, the ΛCDM model is referred to as the standard, fiducial model. The theoretical predictions of the ΛCDM model are in good agreement with current observations, but there are several unresolved problems associated with this model [6].

The main alternatives to the ΛCDM model of dark energy are dynamical scalar field models, in which energy density depends on time [7,8]. In these models, a spatially uniform cosmological scalar field, slowly rolling down its almost flat self-interaction potential, acts

as a time-dependent cosmological constant Λ. In scalar field models, the equation of state (EoS) parameter w_ϕ depends on time: $w_\phi \equiv p_\phi/\rho_\phi$, where p_ϕ and ρ_ϕ are, respectively, the pressure and density energy of the scalar field; on the other hand, in the ΛCDM model, the EoS parameter is a constant: $w_\Lambda = -1$. Depending on the value of the EoS parameter, ϕCDM scalar field models are divided into: quintessence models, with $w_\phi \in (-1, -1/3)$ [9], and phantom models, with $w_\phi < -1$ [10]. Quintessence models are divided into two classes: tracker (freezing) models, in which the scalar field evolves slower than the Hubble expansion rate, and thawing models, in which the scalar field evolves faster than the Hubble expansion rate [11].

We studied a number of ϕCDM scalar field models in order to determine the best dark energy models compared to the ΛCDM model in the present epoch using predicted data from Dark Energy Spectroscopic Instrument (DESI) observations [12,13]. For this purpose, we carried out statistical Bayesian analysis, such as Bayes coefficients, as well as Akaike and Bayesian information criteria. We found that the results of the Bayesian analysis provide compelling evidence in favor of the ΛCDM model. We also conducted Monte Carlo Markov chain (MCMC) analysis and obtained the constraints on the parameters of the scalar field models, comparing the observational data for: the expansion rate of the universe, the angular diameter distance and the growth rate function, with the corresponding data generated for the ΛCDM model.

We investigated how well the Chevallier–Polarsky–Linder (CPL) parametrization approximates the various scalar field models. We determined the location of the scalar field model in the phase space of the CPL parameter. In this manuscript, we used the natural system of units: $c = k_B = 1$.

2. Methods

We considered two types of scalar field ϕCDM model for the spatially flat universe: the quintessence and the phantom scalar field ϕCDM models. We assumed that the flat, homogeneous and isotropic universe is described by the Friedmann–Lemaître–Robertson–Walker spacetime metric, $ds^2 = dt^2 - a^2(t)d\mathbf{x}^2$, where $a(t)$ is the scale factor (normalized to be unity at present epoch $a_0 \equiv a(t_0)$), and t is the cosmic time.

The action and the Klein–Gordon scalar field equation of motion are, respectively

$$S = \frac{M_{pl}^2}{16\pi}\int d^4x\,[\sqrt{-g}(\pm\frac{1}{2}g^{\mu\nu}\,\partial_\mu\phi\partial_\nu\phi - V(\phi))], \tag{1}$$

$$\ddot{\phi} + 3\frac{\dot{a}}{a} \pm \frac{\partial V(\phi)}{\partial\phi} = 0 \tag{2}$$

where M_{pl} is a Planck mass, the "$\pm$" sign corresponds to the quintessence/phantom model, the over-dot denotes a derivative with respect to the cosmic time, $g^{\mu\nu}$ is the background metric, and $V(\phi)$ is the self-interacting potential of the scalar field ϕ.

The energy density ρ_ϕ , pressure p_ϕ and EoS parameter w_ϕ of the scalar field are defined, respectively, as

$$\rho_\phi = \frac{M_{pl}^2}{16\pi}\left(\pm\dot{\phi}^2/2 + V(\phi)\right), \tag{3}$$

$$p_\phi = \frac{M_{pl}^2}{16\pi}\left(\pm\dot{\phi}^2/2 - V(\phi)\right), \tag{4}$$

$$w_\phi = \frac{p_\phi}{\rho_\phi} = \frac{\pm\dot{\phi}^2/2 - V(\phi)}{\pm\dot{\phi}^2/2 + V(\phi)}. \tag{5}$$

The regime of a slowly rolling scalar field, in which $w_\phi \approx -1$, is realized under the condition that the kinetic term is much less than the potential one, i.e., $\left|\pm\dot{\phi}^2/2\right| \ll V(\varphi)$.

The EoS parameter of dark energy models is often represented by the CPL $w_0 - w_a$ parametrization [14,15]

$$w(a) = w_0 + w_a\,(1-a) \tag{6}$$

where $w_0 = w(a=1)$ and $w_a = -a^{-2}\left(\frac{dw}{da}\right)\Big|_{a=1/2}$. The CPL parametrization of the EoS parameter for the standard ΛCDM model has the form: $(w_0,\ w_a) = (-1,\ 0)$.

We studied seven phantom and ten quintessence scalar field φCDM models with corresponding potentials:

The quintessence models

- Ratra–Peebles potential: $V(\phi) = V_0 M_{pl}^2 \phi^{-\alpha},\ \alpha = const > 0$ [7]
- Ferreira–Joyce potential: $V(\phi) = V_0 exp\left(-\lambda\phi/M_{pl}\right),\ \lambda = const > 0$ [16]
- Zlatev–Wang–Steinhardt potential: $V(\phi) = V_0\left(exp\left(M_{pl}/\phi\right) - 1\right)$ [17]
- Sugra potential: $V(\phi) = V_0\phi^{-\chi} exp\left(\gamma\phi^2/M_{pl}^2\right), \chi, \gamma = const > 0$ [18]
- Sahni–Wang potential: $V(\phi) = V_0(\cosh(\varsigma\phi) - 1)^g, \varsigma = const > 0, g = const < 1/2$ [19]
- Barreiro–Copeland–Nunes potential: $V(\phi) = V_0(exp(\nu\phi) + exp(\upsilon\phi));\ \nu,\ \upsilon = const \geq 0$ [20]
- Albrecht–Skordis potential: $V(\phi) = V_0((\phi - B)^2 + A)exp(-\mu\phi), A,\ B = const \geq 0, \mu = const > 0$ [21]
- Urena–Lopez–Matos potential: $V(\phi) = V_0 sinh^m\left(\xi M_{pl}\phi\right), \xi = const > 0, m = const < 0$ [22]
- Inverse exponent potential: $V(\phi) = V_0 exp\left(M_{pl}/\phi\right)$ [23]
- Chang–Scherrer potential: $V(\phi) = V_0(1 + exp(-\tau\phi)), \tau = const > 0$ [24]

The phantom models

- Fifth power potential: $V(\phi) = V_0\phi^5$ [25]
- Inverse square potential: $V(\phi) = V_0\phi^{-2}$ [25]
- Exponent potential: $V(\phi) = V_0 exp(\beta\phi),\ \beta = const > 0$ [25]
- Quadratic potential: $V(\phi) = V_0\phi^2$ [26]
- Gaussian potential: $V(\phi) = V_0(1 - exp(\phi^2/\sigma^2));\ \sigma = const$ [26]
- Pseudo-Nambu-Goldstone boson potential: $V(\phi) = V_0(1 - cos(\phi/k)),\ \kappa = const > 0$ [27]
- Inverse hyperbolic cosine potential: $V(\phi) = V_0\ (cosh(\psi\phi))^{-1},\ \psi = const > 0$ [28]

We carried out MCMC analysis to answer the question: "Is it possible to determine a more preferable scalar field ϕCDM model over the standard ΛCDM model ΛCDM model in the present epoch using the predicted data from DESI observations [29]?"

The MCMC analysis was based on calculated theoretical model prediction values of:

- The normalized Hubble parameter for the spatially flat universe

$$E(z) = H(z)/H_0 = \left(\Omega_{r0}(1+z)^4 + \Omega_{m0}(1+z)^3 + \Omega_\varphi(z)\right)^{1/2}, \tag{7}$$

  where $z = 1/a - 1$ is a redshift; $H(z) = \dot{a}/a$ is a Hubble parameter; H_0 is a Hubble constant; Ω_{r0}, Ω_{m0} and Ω_ϕ are density parameters in the present epoch for radiation, matter and scalar field, respectively.

- The angular diameter distance for the spatially flat universe

$$d_A(z) = \frac{1}{H_0\ (1+z)} \int_0^z \frac{dz'}{E(z')} \tag{8}$$

- The combination of the growth rate of the matter density fluctuations and the matter power spectrum amplitude $f(a)\sigma_8(a)$ for each ϕCDM and ΛCDM model.

The growth rate of the matter density fluctuations is given as: $f(a) = dlnD(a)/dlna$, where $D(a) = \delta(a)/\delta(a_0)$ is the linear growth factor representing the normalized matter density fluctuations $\delta(a)$ per the value of those in the present epoch $\delta(a_0)$. The linear growth factor is evaluated by solving the linear perturbation equation [30]

$$D'' + \left(\frac{3}{a} + \frac{E'}{E}\right)D' - \frac{3\Omega_{m0}}{2a^5E^2}D = 0, \tag{9}$$

where a prime denotes a derivative with respect to the scale factor.

The growth rate of matter density fluctuations $f(a)$ can be parameterized as $f(a) \approx [\Omega_m(a)]^{\gamma(a)}$ [31], where $\Omega_m(a) = \Omega_{m0}a^{-3}/E^2(a)$ is the fractional matter density, and $\gamma(a)$ is the growth index, which, in general, is a time-dependent function.

The growth index $\gamma(a)$ can be parameterized in a scale factor-independent manner, which is known as Linder γ-parametrization [32]

$$\gamma = \begin{cases} 0.55 + 0.05(1 + w_0 + 0.5w_a\ ), \text{ if } w_0 \geq -1; \\ 0.55 + 0.02(1 + w_0 + 0.5w_a\ ), \text{ if } w_0 < -1. \end{cases} \tag{10}$$

The value of γ depends on the characteristics (EoS parameter) of the dark energy model being equal to 0.55 for the ΛCDM model [33].

The matter power spectrum amplitude $\sigma_8(a) = D(a)\sigma_8$, where $\sigma_8 = \sigma_8\ (a_0)$ is the rms linear fluctuation in the mass distribution on the scales $8h^{-1}Mpc$, h is a dimensionless normalized Hubble constant, and $H_0 = 100h\ km\ c^{-1}Mpc^{-1}$. We applied the value of $\sigma_8 = 0.815$ obtained from the Planck 2015 mission [33].

- Our variances correspond to the predicted variances for DESI observations in the redshift range $z \in (0.15,\ 1.85)$.

To obtain the starting points for MCMC analysis, for each quintessence and phantom model, we jointly integrated the Klein–Gordon scalar field equation of motion in Equation (2), Equation (7), and the linear perturbation equation in Equation (9), to obtain a wide range of model parameters and the initial conditions. For each potential, plausible solutions were found, for which the following three criteria had to be fulfilled simultaneously:

1. The transition between the matter and dark energy equality ($\Omega_m = \Omega_\varphi$) happened relatively recently $z \in (0.6,\ 0.8)$;
2. The growth rate of the matter density fluctuations $f(a)$ and fractional matter density $\Omega_m(a)$ are parameterized by Linder γ-parametrization Equation (10);
3. The EoS parameter predicted by the different dark energy models should be in agreement with the expected EoS parameter value in the present epoch (for phantom models, $w_0 < -1$; for the quintessence models, $w_0 \in (-1; -0.75)$, taking into account that for the freezing type, $w_a < 0$, and for the thawing type, $w_a > 0$).

In the result of the MCMC analysis, for each potential, the posteriori ranges of the model parameters and the initial conditions were obtained, which included the prior ranges of the initial conditions and model parameters. We calculated the covariance matrix of $d_A(z)$, $E(z)$, and $f(z)\sigma_8(z)$ measurements following the standard Fisher matrix approach described in Ref. [29]. We assumed 14,000 sq. deg. of sky coverage and wavenumbers up to $k_{max} = 0.2\ Mpc/h$. We also took into account the covariance between measurements within the same redshift bin: $d_A(z)$ and $E(z)$ measurements were negatively correlated by about 40%, while correlations with $f(z)\sigma_8(z)$ were below 10% for all redshift bins.

To evaluate the quality of various models and distinguish them from each other, we applied the obtained posterior ranges of the model parameters and initial conditions to conduct the Bayesian statistics. For this, we calculated the Akaike (*AIC*) [34] and Schwarz (*BIC*) [35] information criteria, as well as the Bayes evidence. The *AIC* and *BIC* are defined, respectively, as

$$AIC = -2ln\mathcal{L}_{max} + 2k, \tag{11}$$

$$BIC = -2ln\mathcal{L}_{max} + kln, \tag{12}$$

where $ln\mathcal{L}_{max} \propto \exp\left(-\chi^2_{min}/2\right)$ is the maximum value of the probability function; N is the number of free parameters; and k is the number of the observations.

The Bayes evidence for the model with a set of parameters **b** is given by the integral

$$\mathcal{E} = \int d^3\boldsymbol{p}\mathcal{P}(\boldsymbol{p}), \tag{13}$$

where $\mathcal{P}$ is the posterior likelihood, which is proportional to the local density of the MCMC points.

We also investigated how the various scalar field models can be approximated by CPL parametrization. To this end, we plotted CPL-ΛCDM 3σ confidence level contours using MCMC technique and displayed on them the largest ranges of the EoS parameter values in the present epoch for each ϕCDM model (see Figure 1). These ranges were obtained for different values of the model parameters or the initial conditions from the prior ranges.

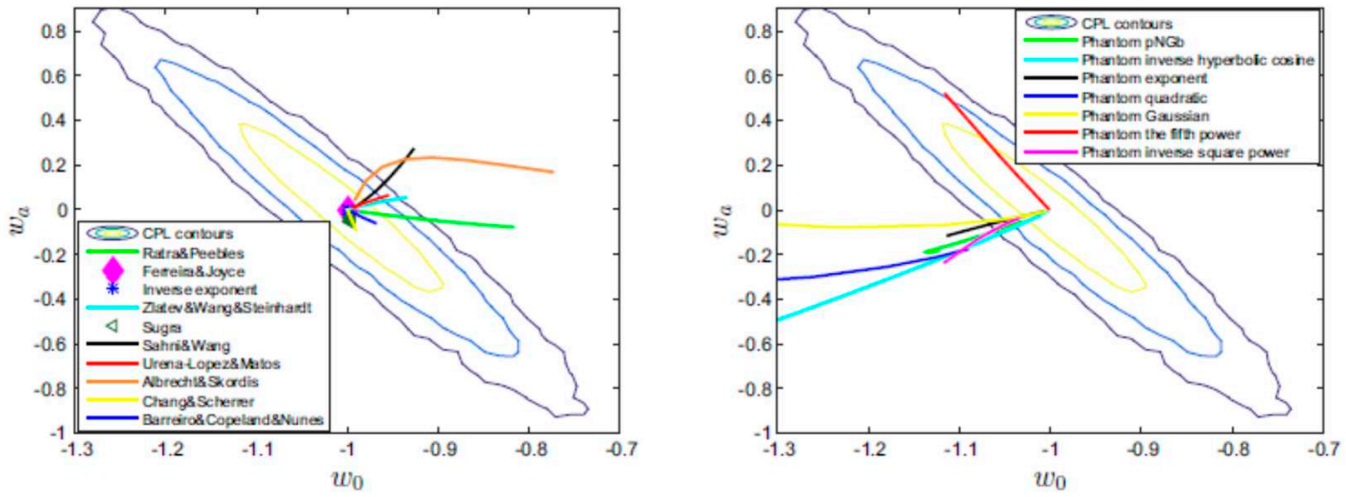

Figure 1. Comparison of the possible (w_0, w_a) values of the quintessence (**left panel**) and phantom (**right panel**) scalar field potentials with CPL-ΛCDM 3σ confidence level contours.

3. Results and Discussion

Upon applying the phenomenological method developed by our group, we reconstructed ten quintessence and seven phantom scalar field ϕCDM models in the spatially flat universe, i.e., we found the prior ranges for the initial conditions and free parameters.

The constraints on dark energy models were obtained by comparing $d_A(z)$, $E(z)$ and $f(z)\sigma_8(z)$ data with the corresponding data generated for the fiducial ΛCDM model using the DESI observations.

For each potential, the posteriori ranges of the model parameters and the initial conditions were obtained, which included the prior ranges of the initial conditions and the model parameters.

We used these posterior ranges to conduct Bayesian statistics. To this end, we calculated the Akaike and Schwarz information criteria, as well as the Bayes evidence. The calculated values of *AIC* and *BIC* and the Bayes factor for all the dark energy models are summarized in Table 1 and in Table 2. These numbers clearly demonstrate that if the ΛCDM model is the true description of dark energy, then the full set of DESI data will be able to strongly discriminate most of the scalar field dark energy models currently under consideration.

Table 1. The list of the scalar field ϕCDM phantom potentials with corresponding *AIC*, *BIC* and Bayes factors values.

Phantom Potential	AIC	BIC	Bayes Factor
$V(\phi) = V_0\phi^5$	10	18.7	0.0921
$V(\phi) = V_0\phi^{-2}$	10	18.7	0.0142
$V(\phi) = V_0 exp(\beta\phi)$	22.4	12	0.0024
$V(\phi) = V_0\phi^2$	10	18.7	0.0808
$V(\phi) = V_0\left(1 - exp\left(\phi^2/\sigma^2\right)\right)$	12	22.4	0.0113
$V(\phi) = V_0(1 - \cos(\phi/\kappa))$	12	22.4	0.0061
$V(\phi) = V_0(cosh(\psi\phi))^{-1}$	12	22.4	0.0056

Table 2. The list of scalar field ϕCDM quintessence potentials with corresponding *AIC*, *BIC* and Bayes factors values.

Quintessence Potential	AIC	BIC	Bayes Factor
$V(\phi) = V_0 M_{pl}^2\phi^{-\alpha}$	10	18.7	0.5293
$V(\phi) = V_0 exp\left(-\lambda\phi/M_{pl}\right)$	12	22.4	0.0059
$V(\phi) = V_0\left(exp\left(M_{pl}/\phi\right) - 1\right)$	10	18.7	0.0067
$V(\phi) = V_0\phi^{-\chi} exp\left(\gamma\phi^2/M_{pl}^2\right)$	14	26.2	0.0016
$V(\phi) = V_0(\cosh(\varsigma\phi) - 1)^g$	14	26.2	0.0012
$V(\phi) = V_0(exp(\nu\phi) + \exp(\upsilon\phi))$	14	26.2	0.0053
$V(\phi) = V_0\left((\phi - B)^2 + A\right)exp(-\mu\phi)$	16	29.9	0.0034
$V(\phi) = V_0 sinh^m\left(\xi M_{pl}\phi\right)$	14	26.2	0.0014
$V(\phi) = V_0 exp\left(M_{pl}/\phi\right)$	10	18.7	0.0077
$V(\phi) = V_0(1 + exp(-\tau\phi))$	12	22.4	0.0024

We investigated how the dark energy models are mapped on the $w_0 - w_a$ phase space of the CPL-ΛCDM contours (see Figure 1).

We found that quintessence models (the Ferreira–Joyce, the inverse exponent, the Sugra, the Chang–Scherrer, the Urena–Lopez–Matos, the Barreiro–Copeland–Nunes and the fifth power phantom model) cannot be distinguished from the ΛCDM model in the present epoch. Whilst quintessence models (the Ratra–Peebles, the Zlatev–Wang–Steinhardt, the Albrecht–Skordis and the Sahni–Wang) and phantom models (the pseudo-Nambu–Goldstone boson, the inverse hyperbolic cosine, the exponent, the Gaussian and the inverse square power) either can be distinguished or cannot be distinguished from the ΛCDM model in the present epoch. The phantom quadratic model can be completely distinguished from the ΛCDM model in the present epoch.

All the studied models can be divided into two types: models whose evolution depends on the values of the initial conditions, and models whose evolution does not depend on the values of the initial conditions. The first type includes the following quintessence models: the Zlatev–Wang–Steinhardt and the Sahni–Wang models, as well as the following phantom models: the quadratic, the Gaussian, the fifth power and the inverse square power. The second type includes the following quintessence models: the Sugra, the Chang–Scherrer, the Albrecht–Skordis, the Urena–Lopez–Matos and the Barreiro–Copeland–Nunes, as well as the following phantom models: the pseudo-Nambu–Goldstone boson, the inverse hyperbolic cosine and the exponent.

4. Conclusions

We investigated ten quintessence and seven phantom scalar field ϕCDM models in the spatially flat universe. We reconstructed these models using the phenomenological method developed by our group.

We carried out constraints of scalar field ϕCDM models using predicted DESI data and conducted MCMC analysis. These constraints were obtained by comparing the normalized Hubble parameter $E(z)$, the angular diameter distance $d_A(z)$, a combination of data on the growth rate of matter density fluctuations and the matter power spectrum amplitude $f(a)\sigma_8(a)$, with corresponding data generated for the fiducial ΛCDM model.

We applied the Bayes statistical criteria to compare the models, such as the Bayes factor, as well as the *AIC* and *BIC* information criteria. Using the Bayesian statistical analysis, we could not uniquely identify the best ϕCDM models compared to the fiducial ΛCDM model based on the predicted DESI data, so the ΛCDM model is a true model.

Upon mapping ϕCDM models in the phase space of the CPL-ΛCDM contours, we could identify the subclasses of these models that, in the present epoch: (i) have attractor solutions and the usual solutions; (ii) can be distinguished from the ΛCDM model; (iii) cannot be distinguished from the ΛCDM model, and (iv) can be either distinguished or undistinguished from the ΛCDM model.

Author Contributions: Conceptualization, O.A. and L.S.; methodology, O.A.; software, L.S.; validation, O.A. and L.S.; formal analysis, O.A. and L.S; investigation, O.A.; resources, O.A.; data curation, L.S.; writing—original draft preparation, O.A.; writing—review and editing, O.A. and L.S.; visualization, O.A.; supervision, L.S. All authors have read and agreed to the published version of the manuscript.

Funding: This research was funded by the Shota Rustaveli National Science Foundation grant #FR-19-8306.

Institutional Review Board Statement: Not applicable.

Informed Consent Statement: Not applicable.

Data Availability Statement: Available in: https://arxiv.org/abs/1711.11465.

Acknowledgments: This study was supported by the Shota Rustaveli National Science Foundation (grant #FR-19-8306).

Conflicts of Interest: The authors declare no conflict of interest.

References

1. Riess, A.G.; Filippenko, A.V.; Challis, P.; Clocchiattia, A.; Diercks, A.; Garnavich, P.M.; Gilliland, R.L.; Hogan, C.J.; Jha, S.; Kirshner, R.P. Observational evidence from supernovae for an accelerating universe and a cosmological constant. *Astron. J.* **1998**, *116*, 1009–1038. [CrossRef]
2. Perlmutter, S.; Aldering, G.; Goldhaber, G.; Knop, R.A.; Nugent, P.; Castro, P.G.; Deustua, S.; Fabbro, S.; Goobar, A.; Groom, D.E. Measurements of Omega and Lambda from 42 high redshift supernovae. *Astrophys. J.* **1999**, *517*, 565–586. [CrossRef]
3. Frieman, J.; Turner, M.; Huterer, D. Dark Energy and the Accelerating Universe. *Ann. Rev. Astron. Astrophys.* **2008**, *46*, 385–432. [CrossRef]
4. Einstein, A. On the General Theory of Relativity. *Sitzungsber. Preuss. Akad. Wiss. Berlin. (Math. Phys.)* **1915**, *1915*, 778–786.
5. Aghanim, N.; Akrami, Y.; Ashdown, M.; Aumont, J.; Baccigalupi, C.; Ballardini, M.; Banday, A.J.; Barreiro, R.B.; Bartolo, N.; Basak, S.; et al. Planck 2018 results. VI. Cosmological parameters. *Astron. Astrophys.* **2020**, *641*, A6.
6. Valentino, E.D. Challenges of the Standard Cosmological Model. *Universe* **2022**, *8*, 399. [CrossRef]
7. Ratra, B.; Peebles, P.J.E. Cosmological Consequences of a Rolling Homogeneous Scalar Field. *Astrophys. J.* **1988**, *325*, L17–L20. [CrossRef] [PubMed]
8. Wetterich, C. Cosmologies with variable Newton's constant. *Nucl. Phys. B* **1988**, *302*, 645–667. [CrossRef]
9. Peebles, P.J.E.; Ratra, B. The Cosmological constant and dark energy. *Rev. Mod. Phys.* **2003**, *75*, 559. [CrossRef]
10. Caldwell, R.R. A Phantom menace? *Phys. Lett. B* **2002**, *545*, 23. [CrossRef]
11. Frampton, P.H.; Ludwick, K.J.; Scherrer, R.J. Pseudo-rip: Cosmological models intermediate between the cosmological constant and the little rip. *Phys. Rev. D* **2011**, *84*, 063003. [CrossRef]
12. Levi, M.; Bebek, C.; Beers, T.; Blum, R.; Cahn, R.; Eisenstein, D.; Flaugher, B.; Honscheid, K.; Kron, R.; Lahav, O.; et al. The DESI Experiment, a whitepaper for Snowmass 2013. *arXiv* **2013**, arXiv:1308.0847.

13. Aghamousa, A.; Aguilar, J.; Ahlen, S.; Alam, S.; Allen, L.E.; Prieto, C.A.; Annis, J.; Bailey, S.; Balland, C.; Ballester, O.; et al. The DESI Experiment Part I: Science, Targeting, and Survey Design. *arXiv* **2016**, arXiv:1611.00036.
14. Chevallier, M.; Polarski, D. Accelerating universes with scaling dark matter. *Int. J. Mod. Phys. D* **2001**, *10*, 213. [CrossRef]
15. Linder, E.V. Exploring the expansion history of the universe. *Phys. Rev. Lett.* **2003**, *90*, 091301. [CrossRef] [PubMed]
16. Ferreira, P.G.; Joyce, M. Cosmology with a primordial scaling field. *Phys. Rev. D* **1998**, *58*, 023503. [CrossRef]
17. Zlatev, I.; Wang, L.M.; Steinhardt, P.J. Quintessence, cosmic coincidence, and the cosmological constant. *Phys. Rev. Lett.* **1999**, *82*, 896. [CrossRef]
18. Brax, P.; Martin, J. Quintessence model building. *Phys. Lett. B* **1999**, *468*, 40. [CrossRef]
19. Sahni, V.; Wang, L.M. A new cosmological model of quintessence and dark matter. *Phys. Rev. D* **2000**, *62*, 103517. [CrossRef]
20. Barreiro, T.; Copeland, E.J.; Nunes, N.J. Quintessence arising from exponential potentials. *Phys. Rev. D* **2000**, *61*, 127301. [CrossRef]
21. Albrecht, A.; Skordis, C. Phenomenology of a realistic accelerating universe using only Planck scale physics. *Phys. Rev. Lett.* **2000**, *84*, 2076. [CrossRef] [PubMed]
22. Urena-Lopez, L.A.; Matos, T. A new cosmological tracker solution for quintessence. *Phys. Rev. D* **2000**, *62*, 081302. [CrossRef]
23. Caldwell, R.R.; Linder, E.V. The limits of quintessence. *Phys. Rev. Lett.* **2005**, *95*, 141301. [CrossRef] [PubMed]
24. Chang, H.Y.; Scherrer, R.J. Reviving Quintessence with an Exponential Potential. *arXiv* **2016**, arXiv:1608.03291.
25. Scherrer, R.J.; Sen, A.A. Phantom Dark Energy Models with a Nearly Flat Potential. *Phys. Rev. D* **2008**, *78*, 067303. [CrossRef]
26. Dutta, S.; Scherrer, R.J. Dark Energy from a Phantom Field Near a Local Potential Minimum. *Phys. Lett. B* **2009**, *676*, 12. [CrossRef]
27. Frieman, J.A.; Hill, C.T.; Stebbins, A.; Waga, I. Cosmology with ultralight pseudo Nambu-Goldstone bosons. *Phys. Rev. Lett.* **1995**, *75*, 2077. [CrossRef]
28. Rakhi, R.; Indulekha, K. Dark Energy and Tracker Solution: A Review. *arXiv* **2009**, arXiv:0910.5406.
29. Font-Ribera, A.; McDonald, P.; Mostek, N.; Reid, B.A.; Seo, H.J.; Slosar, A. DESI and other dark energy experiments in the era of neutrino mass measurements. *J. Cosmol. Astropart. Phys.* **2014**, *1405*, 023. [CrossRef]
30. Wang, L.M.; Steinhardt, P.J. Cluster abundance constraints on quintessence models. *Astrophys. J.* **1998**, *508*, 483. [CrossRef]
31. Linder, E.V.; Cahn, R.N. Parameterized Beyond-Einstein Growth. *Astropart. Phys.* **2007**, *28*, 481. [CrossRef]
32. Pace, F.; Waizmann, J.-C.; Bartelmann, M. Spherical collapse model in dark-energy cosmologies. *Mon. Not. R. Astron. Soc.* **2010**, *406*, 1865. [CrossRef]
33. Ade, P.A.R.; Aghanim, N.; Arnaud, M.; Ashdown, M.; Aumont, J.; Baccigalupi, C.; Banday, A.J.; Barreiro, R.B.; Bartlett, J.G.; Bartolo, N.; et al. Planck 2015 results. XIII. Cosmological parameters. *Astron. Astrophys.* **2016**, *594*, A13.
34. Akaike, H. A new look at the statistical model identification. *IEEE Transl. Autom. Control* **1974**, *19*, 716–723. [CrossRef]
35. Schwarz, G.H. Estimating the dimension of a model. *Ann. Stat.* **1978**, *6*, 461–464. [CrossRef]